AJNR

MR Diffusion Tensor Imaging and Fiber Tracking in Spinal Cord Compression

David Facon, Augustin Ozanne, Pierre Fillard, Jean-François Lepeintre, Caroline Tournoux-Facon and Denis Ducreux

AJNR Am J Neuroradiol 2005, 26 (6) 1587-1594
http://www.ajnr.org/content/26/6/1587

AJNR Am J Neuroradiol 26:1587–1594, June/July 2005

MR Diffusion Tensor Imaging and Fiber Tracking in Spinal Cord Compression

David Facon, Augustin Ozanne, Pierre Fillard, Jean-François Lepeintre, Caroline Tournoux-Facon, and Denis Ducreux

BACKGROUND AND PURPOSE: **Spinal cord damage can result in major functional disability. Alteration of the spinal cord structural integrity can be assessed by using diffusion tensor imaging methods. Our objective is to evaluate the diagnostic accuracy of apparent diffusion coefficient (ADC), fractional anisotropy (FA), and fiber tracking in both acute and slowly progressive spinal cord compressions.**

METHODS: **Fifteen patients with clinical symptoms of acute ($n = 2$) or slowly progressive ($n = 13$) spinal cord compression and 11 healthy volunteers were prospectively selected. We performed T2-weighted fast spin echo (FSE) and diffusion tensor imaging by using a 1.5-T MR scanner. ADC and FA maps were computed. Regions of interest were placed at the cervical, upper and lower thoracic cord levels for the healthy subjects and on the area with abnormal T2-weighted signal intensity in the patients with cord compression. In three patients, we used fiber tracking to locate the areas of cord compression precisely. Data were analyzed by using a mixed model. The sensitivity (SE) and specificity (sp) of imaging (T2, ADC, and FA maps) in the detection of spinal cord abnormality were statistically evaluated.**

RESULTS: **For the healthy subjects, averaged ADC values ranged from 0.96 10^{-3} mm^2/s to 1.05 10^{-3} mm^2/s and averaged FA values ranged from 0.745 to 0.751. Ten patients had decreased FA (0.67 ± 0.087), and one had increased FA values (0.831); only two patients had increased ADC values (1.03 ± 0.177). There was a statistically significant difference in the FA values between volunteers and patients ($P = .012$). FA had a much higher sensitivity (SE = 73.3%) and specificity (sp = 100%) in spinal cord abnormalities detection compared with T2-weighted FSE imaging (se = 46.7%, sp = 100%) and ADC (SE = 13.4%, sp = 80%).**

CONCLUSIONS: **FA has the highest sensitivity and specificity in the detection of acute spinal cord abnormalities. Spinal cord fiber tracking is a useful tool to focus measurements on the compressed spinal cord.**

Acute spinal cord compression due to various diseases such as metastases, abscess, or spondylosis is a major cause of motor dysfunction. Therapy includes surgical decompression or focal radiation therapy. Because clinical outcome is often related to early therapeutic intervention, rapid diagnosis with MR imaging is required. Clinical signs of cord compression include motor and sensory deficits with spinal tract involvement at discrete levels. In such cases, MR shows the mass effect on the spinal cord, which may be associated with abnormal signal intensity on T2-weighted imaging sequences (1). T2-weighted imaging alone, however, has been reported to have a low sensitivity for the detection of acute myelopathy (2), and in general there is a poor prognosis even after therapeutic measures have been taken (3).

Preliminary studies (4–8) previously assessed the feasibility of MR spinal cord studies by using diffusion-weighted imaging (DWI) and diffusion tensor imaging (DTI). DWI is widely used for diagnostic and prognostic purposes in brain acute stroke (9). DTI is a MR technique that evaluates the translation of extracellular water molecules within the white matter fibers (10–12) and enables reconstruction of three-dimensional images in the brain (13–16) and spinal cord (17) of white matter tracts by using specialized fiber tracking algorithms.

It has been reported elsewhere that DTI sequences with computation of the apparent diffusion coeffi-

Received August 19, 2004; accepted after revision October 29.

From the Departments of Neuroradiology (D.F., A.O., D.C.) and Neurosurgery (J.-F.L.), C.H.U. de Bicêtre, Paris XI University, Le Kremlin-Bicêtre, France; Department of Biostatistics (C.T.-F.), Institut Curie, Paris V University, Paris, France; and Department of Computer Science (P.F.), University of North Carolina, Chapel Hill, NC.

Address correspondence to Denis Ducreux, Department of Neuroradiology, CHU de Bicêtre, Paris XI University, 78 rue du Général Leclerc, 94270 Le Kremlin Bicêtre, France.

cient (ADC) parameter are more sensitive in detecting spinal cord abnormalities in cases of chronic compression such as in cervical spondylotic myelopathy, when compared with regular spin-echo T2-weighted sequences (2). In cases of acute spinal cord compression, DTI with fiber tracking may potentially help to define abnormal areas that are undetected on routine T2-weighted imaging.

We hypothesize that fractional anisotropy (FA), a parameter derived from DTI computations and used for fiber tracking, is a more sensitive parameter than ADC in the detection of abnormal areas in spinal cord compression, in both acute and slowly progressive cases.

Methods

Subjects

Fifteen patients (10 men and five women; mean age, 53.9 years) referred to our institution from our neurosurgical emergency unit were prospectively selected between November 2003 and April 2004. Inclusion criteria matched clinical symptoms of acute or slowly progressive spinal cord compressions (focal sensory-motor deficit). Exclusion criteria were previous spine surgery, spine radiation therapy, and contraindication to MR imaging. Spinal cord compression etiologies were degenerative arthritis with disk herniation (six patients [40%]), spondylodiscitis and infectious epidural invasion (five patients [33%]), and vertebral metastasis and epidural involvement (four patients [27%]). Only two patients (13%) had acute onset of symptoms (<1 day)—one patient with metastasis and the other with spondylodiscitis and infectious epidural invasion. The other 13 patients (87%) had a slowly progressive onset (from 3 to >30 days).

As a control group, we enrolled 11 fully informed healthy volunteers (eight men and three women; mean age, 36.7 years) without neurologic disease. Volunteers were members of our medical imaging department. Our MR protocol was approved by our institutional review board, and all patients gave their consent for the study.

MR Imaging Technique

Imaging was performed on a 1.5-T MR imaging system with actively shielded magnetic field gradients (*G* maximum, 40 mT/m). The protocol began with the acquisition of a T2-weighted coronal scout view followed by a sagittal T2-weighted fast spin echo (FSE) sequence (field of view, 39.9 × 39.9 cm; image matrix, 640 × 384; section thickness, 3 mm; TR/TE, 5030/118 ms; echo train length, 23) and a sagittal T1-weighted SE sequence (field of view, 39.9 × 39.9 cm; image matrix, 640 × 384; section thickness, 3 mm; TR/TE, 400/12 ms; echo train length, 3). Axial T2-weighted FSE sections (field of view, 20 × 20 cm; image matrix, 256 × 256; section thickness, 4 mm; TR/TE, 5100/118 ms; echo train length, 23) were set on abnormal T2-weighted areas detected by using the sagittal T2-weighted sequence. Subsequently, a sagittal spin-echo single-shot echo-planar parallel Grappa diffusion-weighted imaging sequence with acceleration factor two and six noncollinear gradient directions was applied with two *b* values ($b = 0$ and 500 seconds/mm^2; field of view, 17.9 × 17.9 cm; image matrix, 128 × 128; 12 sections with section thickness = 3 mm, nominal voxel size, 1.4 × 1.4 × 3 mm; TR/TE, 4600/73 ms). These directions were as follows: [$(1/\sqrt{2}, 0, 1/\sqrt{2})$; $(-1/\sqrt{2}, 0, 1/\sqrt{2})$; $(0, 1/\sqrt{2}, 1/\sqrt{2})$; $(0, 1/\sqrt{2}, -1/\sqrt{2})$; $(1/\sqrt{2}, 1/\sqrt{2}, 0)$; $(-1/\sqrt{2}, 1/\sqrt{2}, 0)$] providing the best precision in the tensor component when six directions are used (18–20). The acquisition time of diffusion-weighted imaging was 2 minutes 10 seconds per patient study. Patients were asked to avoid moving the head or limbs and swallowing during diffusion-weighted imaging.

Image Analysis

Image analysis was performed on a voxel-by-voxel basis by using dedicated software (DPTools [http://fmritools.hd.free.fr]). Before performing the tensor estimation, an unwarping algorithm was applied to the DTI data set to correct distortions related to eddy currents induced by the large diffusion-sensitizing gradients. This algorithm relies on a three-parameter distortion model including scale, shear, and linear translation in the phase-encoding direction (21). The optimal parameters were assessed independently for each section relative to the T2-weighted corresponding image by the maximization of an entropy-related similarity measure called mutual information (22). Following the distortion correction, the diffusion tensor, and, subsequently, the eigen system (with eigen values $\lambda 1$, λ_2, and λ_3) were calculated voxel by voxel by using the method described elsewhere (23). Thus, ADC mean = $(\lambda 1 + \lambda_2 + \lambda_3)/3 = \lambda$ and $FA = \sqrt{\frac{3}{2}} \cdot \frac{\sqrt{(\lambda_1 - \lambda)^2 + (\lambda_2 - \lambda)^2 + (\lambda_3 - \lambda)^2}}{\sqrt{\lambda_1^2 + \lambda_2^2 + \lambda_3^2}}$, were calculated on the basis of formulas that incorporate the tensor elements to generate quantitative parametric ADC and FA maps in healthy volunteers and patients. FA values around 1 are totally anisotropic; FA values around 0 are totally isotropic.

Fiber Tracking Method

In addition to the two-dimensional parametric color maps processed by using previous methods, three-dimensional white matter fiber tracts maps, based on similarities between neighboring voxels in the shape (quantitative diffusion anisotropy measures) and orientation (principal eigenvector map) of the diffusion ellipsoid, were created and coregistered (24–28) on these maps. Because factors affecting the shape of the apparent diffusion tensor in the white matter include the attenuation of fibers, the degree of myelination, the average fibers diameter and the directional similarity of the fibers in the voxel (13, 14), it was possible to access the fiber connectivity as reported elsewhere (13, 16, 29). The algorithm we used (30, 31) was based on an extraction of the principal diffusion direction (PDD) of the tensor field in the regions where the diffusivity was highly linear and a vector-based tracing scheme.

Measurements

In healthy volunteers, ADC and FA measurements were made at three different levels (cervical, C2–C5; high thoracic, T1–T6; and low thoracic, T7–T12) by using regions of interest (averaged surface = 20 mm^2, 10 voxels) located on the spinal cord by using the most accurate *b*0 image then reported to ADC and FA maps. Special attention was paid to avoid CSF partial volume effect, magnetic susceptibility effects, and motion artifacts in region of interest selection. A reference data base was created with pooled ADC and pooled FA spinal cord measurements at different levels.

In patients, two neuroradiologists independently assessed the presence of abnormal hyperintense areas on T2-weighted images by using a signal intensity variation method between remote normal and on the compression site with small region of interest of 10 mm^2 (25 voxels) as follows: DS = (MCS − MNS)/MNS, where DS is signal intensity variation, MCS is averaged signal intensity inside the region of interest on the compression site, and MNS is averaged signal intensity inside the region of interest on the remote normal spinal cord. T2-weighted signal intensity variation (10.2 ± 7.1%) was measured in healthy volunteers at different spine levels (cervical, C2–C5; high thoracic, T1–T6; and low thoracic, T7–T12) and in patients at the normal cord area remote from the compression

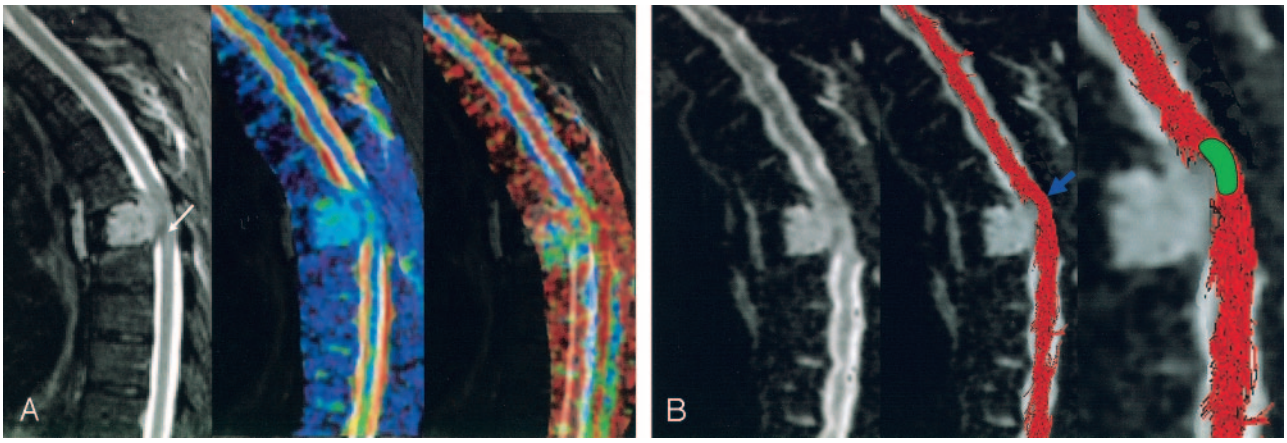

FIG 1. *A,* MR imaging of a spinal cord compression due to a breast tumor metastasis in patient 1. Images are from C7–T10. Color-coded scale related to parameters values. Higher values are coded in red, medium values in green, and lower values in blue. T2-weighted imaging (first image) shows a high signal intensity (*white arrow*), ADC (second image) is slightly increased (*blue-green areas;* ADC = 1.1 10^{-3} mm^2/s versus 0.84 10^{-3} mm^2/s in normal cervicothoracic area) and FA (third image) is decreased (*green areas;* FA = 0.61 vs 0.75 in normal cervicothoracic area) after region of interest measurements. The region of interest in abnormal area was drawn by using the fiber tracking three-dimensional reconstruction.

B, MR imaging of a spinal cord compression due to a breast tumor metastasis with epidural involvement in patient 1. Fiber tracking over *b*0 image shows a mass-effect on fibers tracts. The region of interest (*green area*) was drawn over the maximal level of compression (*blue arrow*) and then automatically reported on the coregistered ADC and FA maps to measure ADC and FA values in the compression site.

site. The compression site was arbitrarily assessed to be hyperintense on T2-weighted images when measurement variation between the normal spinal cord area and the compression site achieved 25%. We chose this ratio as our gold standard for abnormal T2-weighted areas.

The ADC and FA measurements were made at the precise site of compression by using small region of interest of 20 mm^2 (10 voxels) that were exactly located inside the spinal cord on the most accurate b0 image then reported to FA and ADC maps to avoid partial volume effects, magnetic susceptibility effects and motion artifacts. Because of the small regions of interest in patients' compression level spinal cord, we had to compare identical regions of interest to avoid partial volume effect bias. The regions of interest in patients and the healthy volunteers were matched in size.

In three cases, region of interest positioning was difficult to perform because of massive compression of the spinal cord, and we used the fiber tracking (FT) method described above to help us to set the region of interest on the exact site of compression (eg, for patient 1, see Fig 1*A*) on the *b*0 images. FT three-dimensional reconstructions were then coregistered on *b*0 on ADC/FA parametric maps by using our dedicated software (26–28) and showed warped white matter fibers at precise level, thus helping to set region of interest on the exact compression site (see Fig 1*B*).

Statistical Analysis

Analyses were Performed by Using S-Plus 2000 Software (MathSoft, Seattle, WA)

Data of healthy volunteers and patients were described by using mean, standard deviation, median, minimum, and maximum for quantitative variables and the number and percentage for qualitative variables. We first calculated mean FA and ADC for cervical, high thoracic and low thoracic spinal cord levels of the healthy volunteers. We considered spinal cord level as fixed effect and subject as random effect to estimate the effect of the spinal cord levels on FA and ADC. No statistical significant level effect was found for FA and ADC. We pooled the data to set two 95% confidence intervals (one for FA and the other for ADC).

We measured the status effect (volunteer/patient) on FA and ADC of the healthy areas with a mixed model: status (and spinal cord levels if necessary) as fixed effect(s) and subject as random effect. We used a paired *t* test to compare mean FA/ADC values in healthy and pathologic areas. Finally, we calculated sensitivity and specificity of FA, ADC, and T2, with FA and ADC normal values range in the 95% confidence interval.

Results

Patients imaging findings are reported in Table 1, and healthy volunteers results are reported in Table 2. In all patients, imaging findings matched the clinical data (compression level). T2-weighted signal intensity variations, ADC, and FA parameters measurements had a good intra- and interobserver (two neuroradiologists) reproducibility (± 5% in both cases).

In healthy volunteers, normal averaged ADC values ranged from 0.96 10^{-3} mm^2/s to 1.05 10^{-3} mm^2/s (by using a 95% confidence interval). There was no statistically significant level dependence between the three spinal cord measurement sites (cervical and high thoracic, $P = .36$; cervical and low thoracic, $P = .15$), but high thoracic values seemed slightly higher than others. Normal averaged FA values ranged from 0.745 to 0.751 (by using a 95% confidence interval), and there was also no significant level of dependence between the three spinal cord measurement sites (cervical and low thoracic, $P = .86$; high and low thoracic, $P = .67$).

Patients results are reported in Tables 3 and 4. Seven (47%) of 15 patients had abnormal T2-weighted areas at the site of compression. Only two patients (13%) who had degenerative diseases with chronic onset of symptoms had increased ADC values

TABLE 1: Patients' data with estimates of ADC and FA on compression level

Patient (no.)	Sex/Age	Symptoms	IOT	C/ICL	T2 SI	ADC	FA	Diagnoses
1	M/60	MD + Thoracic Pain	7	T9	Normal	1.1	0.61	Metastasis
2	F/80	Thoracic Pain	1	T6	High	1.06	0.831	Metastasis
3	M/59	MD	7	T1–T3	High	0.82	0.78	Metastasis
4	M/76	MD + SD	>30	C1–C2	High	1.41	0.526	Degenerative
5	M/43	MD	15	C6–C7	Normal	1.17	0.73	Degenerative
6	M/62	MD	>30	C5–C7	High	1.26	0.642	Degenerative
7	M/40	SD	>30	T4–T5	Normal	1.03	0.736	Degenerative
8	F/41	Cervical Pain	15	C3–C4	Normal	0.85	0.6	Spondylodiscitis
9	F/46	SD	21	C5–C6	Normal	0.91	0.67	Degenerative
10	F/73	SD	3	T6	High	0.775	0.64	Metastasis
11	M/34	SD + Lumbar Pain	>30	T12–L1	Normal	1.08	0.599	Spondylodiscitis
12	M/77	MD	1	T6–T7	High	1.19	0.8	Spondylodiscitis
13	M/30	MD + SD	>30	C6	Normal	0.97	0.676	Spondylodiscitis
14	F/48	MD	>30	C5–C7	High	0.88	0.614	Spondylodiscitis
15	M/40	MD	21	C4–C5	Normal	1.08	0.6	Degenerative

Note.—Abnormal values are in red. Imaging compression level matched the clinical data.

IOT = imaging/onset time: time between MR exam and onset of symptoms (in days); C/ICL = clinical/imaging compression level; SI = signal intensity; MD = motor deficit; SD = sensitive deficit; ADC = apparent diffusion coefficient ($\times 10^{-3}$ mm^2/s); FA = fractional anisotropy.

TABLE 2: Statistical tests in volunteer

	Average	SD	Median	Minimum	Maximum	MD	*P* Value
FA	0.748	0.027	0.743	0.700	0.800	7	
Cervical	0.748	0.031	0.747	0.700	0.780	1	.86
High thoracic	0.751	0.027	0.740	0.720	0.800	2	.67
Low thoracic	0.745	0.027	0.74	0.714	0.800	4	–
ADC ($\times 10^{-3}$)	1.00	0.130	1.00	0.77	1.25	7	
Cervical	1.01	0.157	1.02	0.77	1.25	1	.36
High thoracic	0.96	0.104	0.93	0.81	1.13	2	–
Low thoracic	1.05	0.111	1.06	0.89	1.19	4	.15

Note.—Comparison of FA and ADC values according to medullar level on healthy volunteers doesn't show a statistically significant difference. SD = standard deviation; MD = patient distribution (number of patients).

TABLE 3: Statistical tests in volunteer

	Average	SD	Median	Minimum	Maximum	MD	*P* Value
FA							.42
Healthy volunteers	0.748	0.027	0.743	0.700	0.800	7	
Patients	0.740	0.034	0.750	0.690	0.780	0	
ADC ($\times 10^{-3}$)							.26
Healthy volunteers	1.00	0.130	1.00	0.77	1.25	7	
Patients	0.949	0.172	0.928	0.730	1.34	0	

Note.—Comparison of FA and ADC of healthy level on healthy volunteers and patients doesn't show a statistically significant difference. SD = standard deviation; MD = patient distribution (number of patients).

(Table 1). Eleven patients (73%) had abnormal FA values at the compression site: 10 patients had decreased FA values (four spondylodiscitis, four degenerative, and two metastases), and one patient had increased FA values (metastasis with acute onset). Averaged FA values varied over time, with initial decreasing values from day 1 to 21, then increasing values from day 21 to 30 (see Fig 2).

There was no statistically significant difference between ADC (P = .42) and FA (P = .26) measurements performed in healthy volunteers and in patients away from the compression site (Table 3). There was a statistically significant difference for FA between healthy volunteer and the patients at the compression site (P = .012), but not for ADC (P = .13; Table 4). FA had a far better sensitivity (SE = 73.3%) and specificity (sp = 100%) in detection of acute spinal cord abnormalities compared with conventional T2-weighted imaging (SE = 46.7%; sp = 100%) or ADC (SE = 13.4%, sp = 80%).

Fiber tracking performed on the spinal cord showed the main white matter tracts (posterolateral corticospinal tracts and posterior lemniscal tracts) in all healthy volunteers and patients (Fig 3). There were some gaps in three-dimensional reconstructions due to artifacts visible on the original DTI images ("hole" ef-

TABLE 4: Statistical tests in volunteer

	Average	SD	Median	Minimum	Maximum	MD	*P* Value
FA							.012
Healthy level	0.740	0.034	0.750	0.690	0.780	0	
Pathologic	0.670	0.087	0.642	0.526	0.831	0	
ADC ($\times 10^{-3}$)							.13
Healthy level	0.949	0.172	0.928	0.730	1.34	0	
Pathologic	1.03	0.177	1.03	0.775	1.41	0	

Note.—Comparison of FA and ADC of pathologic and healthy levels in patients doesn't show a statistically significant difference for ADC but shows one for FA (bold value). SD = standard deviation; MD = patient distribution (number of patients).

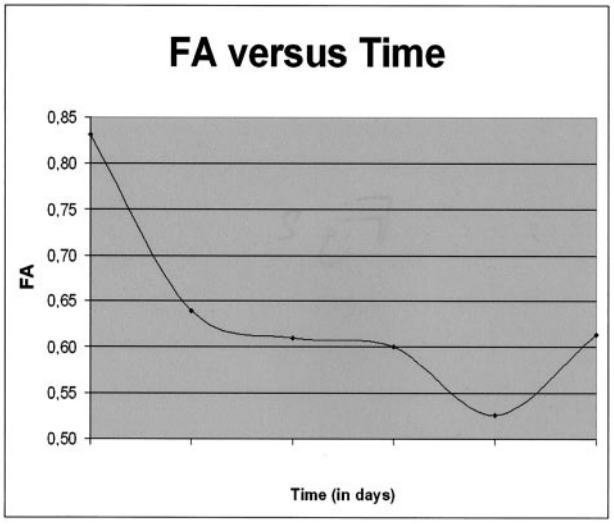

FIG 2. Time course from d1 to d30 of the averaged FA parameter estimated from the compression sites in 11 patients with abnormal FA values. FA values decreased from the 1st to the 21st days, then slightly increased, both related to the extracellular water diffusivity: restricted diffusivity in acute stage and increased diffusivity in chronic stage. Normal values range from 0.69 to 0.8.

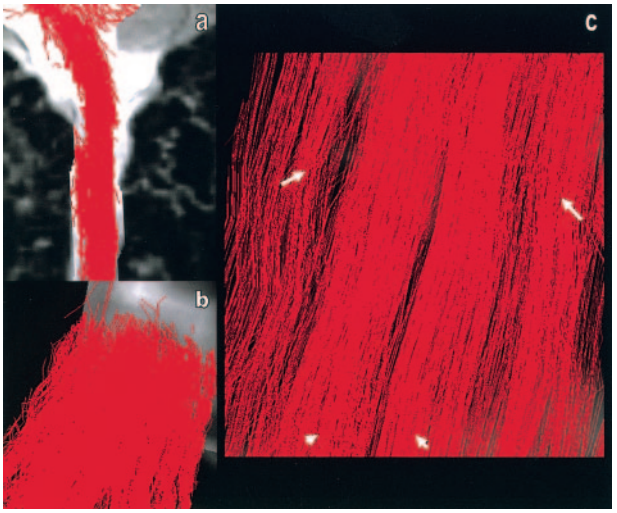

FIG 3. Fiber tracking performed on a volunteer's cervical spinal cord. Sagittal (*A*), axial (*B*), and coronal (*C*) views show tracts reconstructed over the *b*0 sequence. Main white matter tracts are visible on axial (*B*) and coronal (*C*) views of the three-dimensional reconstructions: two individualized posterior lemniscal tracts (*arrowheads*), and posterolateral corticospinal tracts (*arrows*). Other tracts are visible, but have to be more correlated with known anatomy.

fects; Fig 4). In all patients, FT showed the compression sites, matching those seen on the T2-weighted imaging, with mass effect on fiber tracts (Fig 1*B*).

We were able to perform control MR imaging in only six patients. One of them, who had high signal intensity T2 and normal FA (0.78), had a good clinical outcome after surgical decompression. The other one who had high signal intensity T2 and decreased FA (0.64) had residual sensory deficit after surgery. The other four received medical treatment (antibiotherapy) without surgical decompression and also had residual sensory-motor deficit.

Discussion

The diagnosis of acute spinal cord compression is usually assessed clinically. MR imaging shows the mass effect at precise level involving the spinal canal and sometimes reveals abnormal T2-weighted areas inside the cord. This T2-weighted sign is inconstant, appears late—especially in patients with chronic onset of symptoms—and has been reported elsewhere to have a low sensitivity index for the detection of spinal cord myelopathies (1, 3). On the other hand, DWI sequences used in brain acute diseases such as stroke, abscess, or tumors (9) and performed in spinal cord diseases have been reported to improve the diagnostic sensitivity of chronic spinal abnormalities (2, 32). Only two parameters that derive from DWI and DTI MR images, ADC and ADT—which also measure anisotropy (2)—have been studied on these chronic compressions. FA variations in acute and slowly progressive spinal cord compression have not been previously studied, despite the fact that FA parameter is taking advantage of a better directional evaluation of water diffusivity (because of its scalar information) in abnormal areas as previously reported in brain diseases (19).

In our study, we investigated the use of these two parameters in acute and slowly progressive spinal cord compression and evaluated their statistical accuracy in detecting abnormal areas. First we measured the ADC and FA values at different spine levels to confirm the physiologic hypothesis that inner spinal water inflow and outflow may vary depending on cord level (because of spinal vascular anatomy variations) and may then modify normal ADC and FA values measured at these levels (33). Physiologic hydrov-

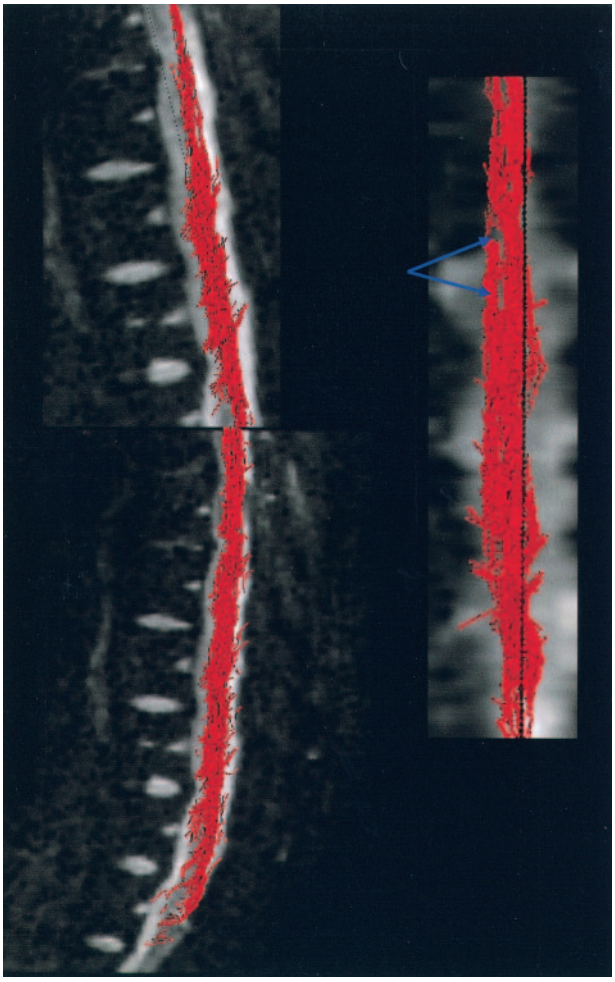

FIG 4. Three-dimensional reconstructions are mapped over the *b*0 images. Fiber tracking performed on the spinal cord volunteer shows some pitfalls of the FT method due to magnetic susceptibility effect of the DTI MR image: "hole" effect, gap in three-dimensional reconstruction (*blue arrows*).

enous flow modifications along the spine cord should interfere with water diffusivity variation, although it has not yet been published.

We found no detectable variation of ADC and FA values at the different cord levels. ADC values of the study ranged were similar to those previously reported in the literature—ranging from 1.03 10–3 to 1.29 10–3 mm^2/s (10)—regarding the fact that they were reported in each principal direction (ADCxx, ADCyy, ADCzz) and that we reported only mean ADC values measured in three different levels, which were equivalent to (ADCxx + ADCyy + ADCzz)/3 (4).

With regard to FA values, previous investigations studied only cervical spine in healthy volunteers (4, 5) and reported values ranged from 0.52 to 0.83 (5, 8). We matched and completed these results by extending to the thoracic spine.

With regard to regions of interest, we had to pay special attention to avoid partial volume effects with the surrounding CSF—it may decrease the FA values if included. Spine and CSF segmentation algorithm should accelerate these measurements and reduce partial volume effect pitfall of the region of interest method. Unfortunately, we lacked such software and had to draw regions of interest manually over gray and white matter if patients had tight spinal cords. To have comparable results, we had to perform in all patients and volunteers similar region of interest positioning (in both gray and white matter), so the values we reported are gray and white averaged values. Spinal white matter fibers have a crania-caudal orientation, so they are very anisotropic. By contrast, gray matter is more isotropic. FA values reflect global anisotropy of the analyzed structure. The closer to one the FA value is, the more anisotropic is this structure. Our results matched the reported animal values—average of the 0.92 white and 0.59 gray matter (34).

We found no evidence of physiologic water in-/outflow variation along the cord, perhaps because of the small sample size of healthy volunteers included in our study and/or the bad quality of some DTI images degraded by artifacts. Larger studies would certainly help clarify this hypothesis.

In our study, the ADC parameter has low sensitivity and specificity in detection of warped spine fibers, even worse than regular T2-weighted imaging. This does not match previously reported results in cervical myelomalacia (2), although the myelomalacia study focused only on cervical degenerative chronic (or slowly progressive) cord compressions. In our study, only two patients with symptomatic chronic degenerative diseases had increased ADC values, which suggests that ADC parameter should only be used for evaluation of chronic spinal cord compression. Poor sensitivity and specificity may be explained by partial evaluation of the water diffusivity, which failed to detect water in-/outflow inside and around the spinal cord fibers.

On the other hand, FA parameter has higher sensitivity and specificity to detect abnormal areas inside the cord, compared with conventional T2-weighted imaging. This is likely the result of complete evaluation of the water diffusivity by using scalar properties of the DTI sequence. Most patients had decreased FA values, which suggests either local extracellular edema or decreased number of fibers increasing extracellular space, or both, as reported elsewhere in brain diseases (9). Experimental studies on spinal cord compressions in rats found decreased FA values due to various elements: mechanical disruption, tearing of fibers and myelin sheaths, extracellular edema, Wallerian degeneration, demyelination, loss of spatial organization, liquefaction, or cystic degeneration (35). In that study, spinal cord compression was experimentally designed and imaged several months after the onset. This allowed them to observe late demyelination and Wallerian degenerative processes that, of course, could not be observed in our study. Their pathophysiologic findings only partially matched ours because of a different time pattern: we studied acute and slowly progressive compressions, and they imaged only chronic compressions. What we

observed may be an increased extracellular space due to acute edema in acute compression stages—that is, Wallerian degeneration and demyelination occurring much later. Our findings suggest a specific time pattern of the FA variations, with acute increased values—due to restricted diffusivity—and late decreased values—due to increased diffusivity in the extracellular space (Fig 2). Nevertheless we observed in one case of acute compression increased FA values. This has never been reported even in experimental studies but may have been caused by early modification of the extracellular compartment, as reported in brain diseases (9). These data suggest either intracellular edema with inflow of the extracellular water or decreased extracellular space, secondary to inflammatory or tumoral cellular infiltration or mechanical compression. Previous studies reported a time pattern of ADC variation in acute stroke: early decreased ADC, which suggested cytotoxic edema characterized by intracellular water inflow, followed by cell lysis, water outflow, and increased ADC, which suggested vasogenic edema. There should exist a similar time gradient of water variation in spinal cord compression, with early decreased and late increased extra cellular space that match the water exchanges around the cell. These findings may be clarified by larger studies.

Finally, experimental studies (35) have suggested the use of FA parameter as a response evaluation after neuroprotective therapy. We observed a good recovery in one patient with normal early FA values and a bad clinical outcome even after surgical decompression in one patient with decreased early FA values. This suggests FA may be a good prognostic parameter in assessing clinical outcome after acute compression. We have insufficient data to assess a relationship between FA values and prognosis, but the hypothesis of a recovery gradient can be reasonably inferred regarding FA values and clinical outcome: poor outcome in cases of markedly decreased FA values and intermediary recovery in cases of slightly decreased FA values. Early increased values reflect an acute compression that may also be of good prognosis if emergency surgery is performed. This hypothesis needs to be evaluated in larger studies.

With regard to fiber tracking, this tool seems to be more than just a visualization tool for the white matter tracts of the spinal cord. Anatomic correlation to corticospinal and spinothalamic pathways is excellent. Fiber tracking can demonstrate specific white matter tracts involved by mass effect and may help assess the positive diagnosis of spinal cord abnormalities by locating specifically the area involved by compression. This technique needs to be improved, however, to avoid the "hole" effects observed on three-dimensional reconstructions. They are due to the small spinal cord diameter, with CSF flow, respiratory, and cardiac motion artifacts that may decrease the image quality by inducing magnetic susceptibility artifacts (even with the Grappa parallel imaging we used). It may be corrected by using a better coregisteration algorithm that corrects for more motion artifacts compared with ours (26–28) and by using more gradient directions in DTI sequences. DTI research studies in the brain are performed by using >25 gradient directions (36). Adding gradient directions may help improve the scalar sampling of the water diffusivity and may correct this artifact (36). Unfortunately, we were not able to verify this assumption because of the six-DTI-direction limitation of our MR scanner. Despite these pitfalls, images we obtained had sufficient quality to analyze ADC and FA variations in acute and slowly progressive (chronic) spine compressions. In addition, fiber tracking enabled us to locate the precise site of compression on the white matter tracts (Fig 1).

Conclusion

We conclude that FA is more sensitive than ADC and T2-weighted imaging in detecting spinal cord abnormalities in patients with acute and slowly progressive cord compression. This parameter derived from DTI MR images may be a prognostic factor for the patient's clinical outcome after treatment, but larger studies are needed to confirm this hypothesis. Spinal cord fiber tracking is able to visualize the major spinal cord main white matter tracts and may help in the MR assessment of acute or slowly progressive cord compression by showing involved areas that are otherwise invisible.

Acknowledgments

We would specially like to thank Professor Pierre Lasjaunias, Dr. Jean-Luc Sarrazin, Dr. Kathlyn Marsot-Dupuch, Dr. Marie-Christine Petit-Lacour, Dr. Farida Benoudiba, Dr. Trung Duong, and Dr. Soke-Miang Chng, for their precious help and support.

References

1. Takahashi M, Yamashita Y, Sakamoto Y, Kojima R. **Chronic cervical cord compression: clinical significance of increased signal intensity on MR images.** *Radiology* 1989;173:219–224
2. Demir A, Ries M, Moonen C, et al. **Diffusion-weighted MR imaging with apparent diffusion coefficient and apparent diffusion tensor maps in cervical spondylotic myelopathy.** *Radiology* 2003;229:37–43
3. Matsumoto M, Toyama Y, Ishikawa M, et al. **Increased signal intensity of the spinal cord on magnetic resonance images in cervical compressive myelopathy.** *Spine* 2000;25:677–682
4. Holder C, Muthupillai R, Mukundan S, et al. **Diffusion-weighted MR Imaging of the normal human spinal cord in vivo.** *AJNR Am J Neuroradiol* 2000;21:1799–1806
5. Ries M, Jones R, Dousset V, Moonen C. **Diffusion tensor MRI of the spinal cord.** *Magn Reson Med* 2000;44:884–892
6. Clark C, Werring D, Miller D. **Diffusion imaging of the spinal cord in vivo: estimation of the principal diffusivities and application to multiple sclerosis.** *Magn Reson Med* 2000;43:133–138
7. Bammer R, Fazekas F, Augustin M, et al. **Diffusion-weighted MR imaging of the spinal cord.** *AJNR Am J Neuroradiol* 2000;21:587–591
8. Cercignani M, Horsfield M, Agosta F, Filippi M. **Sensitivity-encoded diffusion tensor MR imaging of the cervical cord.** *AJNR Am J Neuroradiol* 2003;24:1254–1256
9. Le Bihan D. **Diffusion and perfusion magnetic resonance imaging.** New York: Raven Press;1995:chap A-2-IV, pp 50–57
10. LeBihan D. **Molecular diffusion nuclear magnetic resonance imaging.** *Magn Reson Q* 1991;7:1–30
11. Basser P, Mattiello J, LeBihan D. **MR diffusion tensor spectroscopy and imaging.** *Biophys J* 1994B;66:259–267

12. Basser P, Pierpaoli C. **Microstructural and physiological features of tissues elucidated by quantitative-diffusion-tensor MRI.** *J Magn Reson* 1996;111:209–219
13. Basser PJ. **Fiber-tractography via diffusion tensor MRI (DTMRI).** In the proceedings of the VIth annual meeting of the International Society of Magnetic Resonance in Medicine. 1998: Sydney, Australia; 1226
14. Conturo TE, Lori NF, Cull TS, et al. **Tracking neuronal fiber pathways in the living human brain. Proc Natl Acad Sci U S A.** 1999;96:10422–10427
15. Mori S, Crain BJ, Chacko VP, Van Zijl PCM. **Three-dimensional tracking of axonal projections in the brain by magnetic resonance imaging.** *Ann Neurol* 1999;45:265–269
16. Poupon C, Mangin JF, Pachot-Clouard M, et al. **Tracking fiber bundles in diffusion tensor images.** *Neuroimage* 1998B;7:701
17. Wheeler-Kingshott C, Hickman S, Parker G, et al. **Investigating cervical spinal cord structure using axial diffusion tensor imaging.** *Neuroimage* 2002;16:93–102
18. Pierpaoli C, Basser PJ. **Toward a quantitative assessment of diffusion anisotropy.** *Magn Reson Med* 1996;36:893–906
19. Pierpaoli C, Jezzard P, Basser PJ, Barnett A, DiChiro G. **Diffusion tensor MR imaging of the human brain.** *Radiology* 1996;201:637–648
20. Basser P, Pierpaoli C. **A Simplified method to measure the diffusion tensor from seven MR images.** *Magn Reson Med* 1998;39:928–934
21. Haselgrove JC, Moore JR. **Correction of distortion of echo-planar images used to calculate the apparent diffusion coefficient.** *Magn Reson Med* 1996;36:960–964
22. Poupon C, Clark CA, Frouin V, et al. **Regularization of diffusion-based direction maps for the tracking of brain white matter fascicles.** *Neuroimage* 2000;12:184–195
23. Basser P, Mattiello J, LeBihan D. **Estimation of the effective self-diffusion tensor from the NMR spin echo.** *J Magn Reson* 1994A;103:247–254
24. Ulug AM, Van Zijl PCM. **Orientation-independent diffusion imaging without tensor diagonalization: anisotropy definition based on physical attributes of the diffusion ellipsoid.** *J Magn Reson Imaging* 1999;9:804–813
25. Alexander AL, Hasan K, Kindlmann G, et al. **A geometric analysis of diffusion tensor measurements of the human brain.** *Magn Reson Med* 2000;44:283–291
26. Woods RP, Cherry SR, Mazziotta JC. **Rapid automated algorithm for aligning and reslicing PET images.** *J Comput Assist Tomogr* 1992;16:620–633
27. Woods RP, Grafton ST, Holmes CJ, et al. **Automated image registration: I. General methods and intrasubject, intramodality validation.** *J Comput Assist Tomogr* 1998;22:141–154
28. Woods RP, Grafton ST, Watson JDG, et al. **Automated image registration: II. Intersubject validation of linear and nonlinear models.** *J Comput Assist Tomogr* 1998;22:155–165
29. Jones DK, Simmons A, Williams SCR, Horsfield MA. **Non-invasive assessment of axonal fiber connectivity in the human brain via diffusion tensor MRI.** *Magn Reson Med* 1999;42:37–41
30. Westin CF, Maier SE, Mamata H, et al. **Processing and visualization for diffusion tensor MRI.** *Med Image Anal* 2002;6:93–108
31. Xu D, Mori S, Solaiyappan M, et al. **A framework for callosal fiber distribution analysis.** *Neuroimage* 2002;17:1131–1143
32. Tsichiya K, Katase S, Fujikawa A, et al. **Diffusion-weighted MRI of the cervical spinal cord using a single-shot fast spin-echo technique: findings in normal subjects and in myelomalacia.** *Neuroradiology* 2003;45:90–94
33. Lasjaunias P, Berenstein A, Ter Brugge KG. **Spinal and spinal cord arteries and veins.** In: *Surgical neuroangiography.* Berlin: Springer-Verlag;2001:146–164
34. Elshafiey I, Bilgen M, He R, Narayana P. **In vivo diffusion tensor imaging of rat spinal cord at 7 T.** *Magn Reson Imag* 2002;20:243–247
35. Nevo U, Hauben E, Yoles E, et al. **Diffusion anisotropy MRI for quantitative assessment of recovery in injured rat spinal cord.** *Magn Reson Med* 2001;45:1–9
36. Jones DK. **The effect of gradient sampling schemes on measures derived from diffusion tensor MRI: a Monte Carlo study.** *Magn Reson Med* 2004;51:807–815